



Design of Ga–DOTA-based bifunctional radiopharmaceuticals: Two functional moieties can be conjugated to radiogallium–DOTA without reducing the complex stability

Takahiro Mukai*, Jun Suwada, Kohei Sano, Mayumi Okada, Fumihiko Yamamoto, Minoru Maeda

Department of Biomolecular Recognition Chemistry, Graduate School of Pharmaceutical Sciences, Kyushu University, 3-1-1 Maidashi, Higashi-ku, Fukuoka 812-8582, Japan

ARTICLE INFO

Article history:

Received 18 March 2009
Revised 13 May 2009
Accepted 14 May 2009
Available online 21 May 2009

Keywords:

Radiogallium
DOTA
Bifunctional radiopharmaceuticals
Metronidazole
Hypoxia

ABSTRACT

From the X-ray crystal structures of Ga–DOTA chelates, we were able to deduce that two free carboxylate groups of the radiogallium–DOTA complex may be utilized for coupling to functional moieties that recognize molecular targets for in vivo imaging without reducing the radiogallium–complex stability. Thus, we designed 2,2'-[4,10-bis(2-[[2-(2-methyl-5-nitro-1H-imidazol-1-yl)ethyl]amino]-2-oxoethyl)-1,4,7,10-tetraazacyclododecane-1,7-diy]diacetic acid (DOTA-MN2) (**7**), employing a metronidazole moiety as the recognition site of hypoxic lesions, based on the drug design concept of bifunctional radiopharmaceuticals. Coupling of DOTA-bis(*tert*-butyl)ester **5** with 1-(2-aminoethyl)-2-methyl-5-nitroimidazole dihydrochloride, followed by deprotection, afforded the required **7** (DOTA-MN2). ⁶⁷Ga-labeling was carried out by reaction of DOTA-MN2 with ⁶⁷Ga-citrate. When ⁶⁷Ga–DOTA-MN2 was incubated in phosphate-buffered saline or mouse plasma, no measurable decomposition occurred over a 24-h period. In biodistribution experiments in NFSa tumor-bearing mice, ⁶⁷Ga–DOTA-MN2 displayed not only a significant tumor uptake, but also rapid blood clearance and low accumulations in nontarget tissues, resulting in high target-to-nontarget ratios of radioactivity. These results indicate the potential benefits of the drug design of ⁶⁷Ga–DOTA-MN2. The present findings provide helpful information for the development of radiogallium-labeled radiopharmaceuticals for SPECT and PET studies.

© 2009 Elsevier Ltd. All rights reserved.

1. Introduction

Positron emission tomography (PET) is a noninvasive medical imaging technology that can be used to image the distribution of positron-emitter-labeled agents with high resolution and sensitivity. As positron-emitters for PET, ¹¹C, ¹³N, ¹⁵O and ¹⁸F have been widely used, but their physical half-lives are very short (¹¹C: 20.39 min, ¹³N: 9.96 min, ¹⁵O: 122 s, ¹⁸F: 109.8 min). Thus, the use of PET requires large-scale and expensive equipment such as an on-site cyclotron for the production of the short-lived positron-emitters, radiochemistry systems for the synthesis of PET tracers, and incidental equipment, limiting the availability of PET imaging.^{1,2}

Similar to a γ -emitter produced by ⁹⁹Mo/^{99m}Tc generator, ^{99m}Tc, which is still the mainstay of diagnostic nuclear medicine, generator-produced positron-emitters are expected to contribute to the progress of available PET studies.^{3,4} Among them, a metallic radionuclide, ⁶⁸Ga is of great interest because of its radiophysical properties ($t_{1/2}$ = 68 min; β^+ = 89% and EC = 11%; E_{β^+max} = 1899 MeV).^{5–9} The long half-life of the parent ⁶⁸Ge ($t_{1/2}$ = 270.8 days) permits

shipping of ⁶⁸Ge/⁶⁸Ga generators to a clinical site from which the daughter ⁶⁸Ga can be eluted on-site at any time on demand. Despite these advantages, there are few recent publications on the development of ⁶⁸Ga-labeled compounds except for ⁶⁸Ga-labeled peptides and proteins while a large number of ^{99m}Tc-labeled compounds have been developed and used clinically. The development of ⁶⁸Ga-labeled compounds may be hampered by a lack of knowledge of radiogallium-labeling chemistry.

1,4,7,10-Tetraazacyclododecane-1,4,7,10-tetraacetic acid (DOTA) is well used as a chelator to form stable complexes with radiometals. This ligand has eight coordinating donor atoms (four nitrogens and four oxygens) and forms octa-coordinated complexes with metals in +3 oxidation state.¹⁰ However, recent crystallographic studies demonstrated a hepta-coordinated structure of Ga–DOTA complexes; the four nitrogens of the cyclen ring and two oxygens of the opposite carboxylate arms are coordinated to the metal.^{11,12} From these observations, we were able to deduce that two free carboxylate groups of the radiogallium–DOTA complex should be utilized for coupling to functional moieties that recognize molecular targets for in vivo imaging without reducing the radiogallium–complex stability.

To test this idea, we planned the development of a two functional moieties-conjugated Ga–DOTA chelate, based on the concept

* Corresponding author. Tel.: +81 92 642 6651; fax: +81 92 642 6654.
E-mail address: mukai@phar.kyushu-u.ac.jp (T. Mukai).

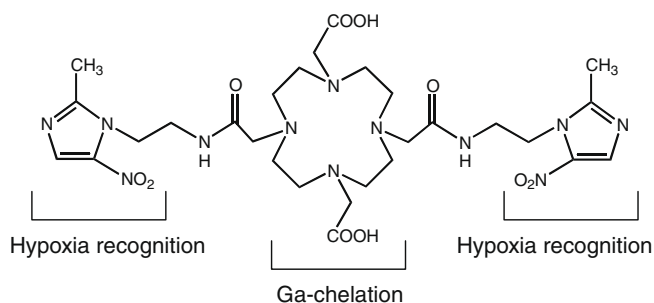


Figure 1. Chemical structure of a bifunctional radiopharmaceutical, DOTA-MN2 (7).

of bifunctional radiopharmaceuticals. Bifunctional radiopharmaceuticals have the recognition site of the molecular target and chelation site for the radiometal independently in one molecule.^{13–16} In the present study, we designed and synthesized 2,2'-[4,10-bis(2-[[2-(2-methyl-5-nitro-1H-imidazol-1-yl)ethyl]amino)-2-oxoethyl]-1,4,7,10-tetraazacyclododecane-1,7-diyl]diacetic acid (Fig. 1, DOTA-MN2), employing a metronidazole moiety as the recognition site of hypoxic lesions. To validate the utility of the drug design, DOTA-MN2 was labeled with the easy-to-handle radioisotope, ⁶⁷Ga, and its in vitro stability and biodistribution in mice were assessed.

2. Results and discussion

2.1. Chemistry

The key step for the preparation of DOTA-bis-ester, a precursor of DOTA-MN2, is regioselective N-deprotection of cyclen. At first, N1,N7-di-protection of cyclen was performed by reaction with benzyl chloroformate in aqueous media under strict pH control between 2 and 3, according to the method reported by Kovacs and Sherry.¹⁷ While our study was in progress, León-Rodríguez et al. reported the synthesis of N1,N7-di-protected cyclen **1** using *tert*-bu-

tyl-(oxycarbonyloxy)succinimide.¹⁸ Using this approach, as outlined in Figure 2, DOTA-bis(*tert*-butyl)ester **5** was obtained in good yields (82%). Acid-amine coupling of **5** with 1-(2-aminoethyl)-2-methyl-5-nitroimidazole dihydrochloride in the presence of 1-hydroxybenzotriazole (HOBT), 1-ethyl-3-[3-(dimethylamino)propyl] carbodiimide hydrochloride (EDC), and triethylamine in a mixed solvent of CH₂Cl₂ and DMF gave **6** in 34% yield. Hydrolysis of **6** with hydrochloric acid afforded the required **7** (DOTA-MN2) in 95% yield. The ¹H NMR and MS spectra were consistent with the assigned structures.

A nonradioactive gallium-complex, Ga-DOTA-MN2 was prepared by reacting DOTA-MN2 with Ga(NO₃)₃·nH₂O in 0.2 M ammonium acetate buffer (pH 4.6). Heating was needed to complete the reaction. In HPLC analyses, Ga-DOTA-MN2 and DOTA-MN2 showed well-separated peaks as shown in Figure 3. The structure of Ga-DOTA-MN2 was assigned by ESI MS although the crystal structure could not be determined. ⁶⁷Ga-labeling was carried out by reaction of DOTA-MN2 with ⁶⁷Ga-citrate in an ammonium acetate buffer (pH 5.8) at 95 °C. After purification by HPLC, ⁶⁷Ga-DOTA-MN2 was obtained with high radiochemical purity (over 96%) as determined by HPLC, cellulose acetate electrophoresis and cellulose F TLC. Radiochemical yields of the final formulated product were 35–59%.

2.2. Biological studies

The stability of ⁶⁷Ga-DOTA-MN2 was investigated by incubation with phosphate-buffered saline (pH 7.4) or mouse plasma at 37 °C (Table 1). In both cases, the radiochemical purities of ⁶⁷Ga-DOTA-MN2 were unchanged for 24 h. These results indicate that ⁶⁷Ga-DOTA-MN2 is highly stable in vitro although two carboxylates in the DOTA skeleton are conjugated with metronidazole derivatives.

To assess the radioactivity pharmacokinetics, ⁶⁷Ga-DOTA-MN2 was administered to normal mice (Table 2). At 30 min post-injection, the blood radioactivity was already at markedly low levels, showing a fast blood clearance of ⁶⁷Ga-DOTA-MN2. Only low radioactivity, amounting to less than 0.9% of the injected dose/g,

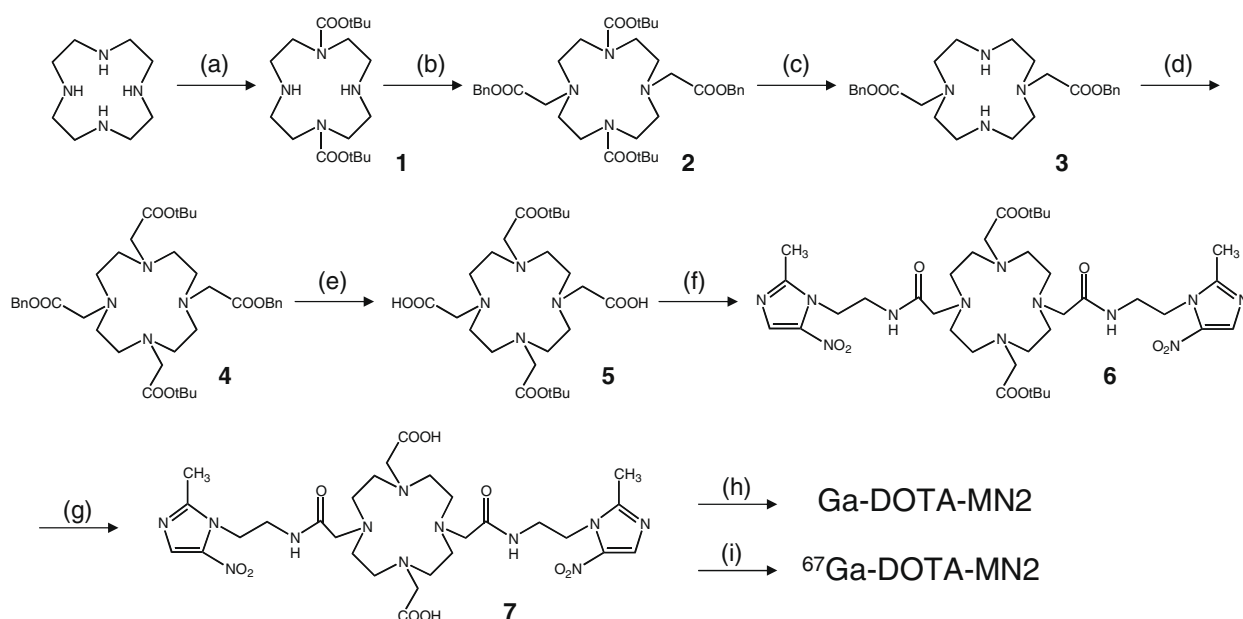


Figure 2. Synthesis of DOTA-MN2. Reagents and conditions: (a) *tert*-butyl-(oxycarbonyloxy)succinimide, CHCl₃ (quant.); (b) benzyl bromoacetate, K₂CO₃, acetonitrile (91.7%); (c) TFA, CH₂Cl₂ (97.0%); (d) *tert*-butyl bromoacetate, K₂CO₃, acetonitrile (92.7%); (e) Pd/C, H₂, ethanol (quant.); (f) 1-(2-aminoethyl)-2-methyl-5-nitroimidazole dihydrochloride, HOBT, EDC, triethylamine, CH₂Cl₂, DMF (33.9%); (g) concd HCl (95.4%); (h) Ga(NO₃)₃·nH₂O, 0.2 M NH₄OAc buffer (pH 4.6); (i) ⁶⁷Ga-citrate, 0.2 M NH₄OAc buffer (pH 5.8).

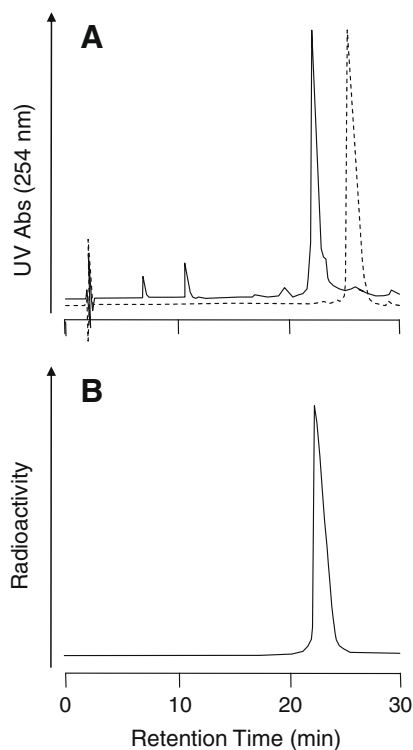


Figure 3. Typical HPLC profiles of Ga-DOTA-MN2 (solid line) and DOTA-MN2 (broken line) (A) and ^{67}Ga -DOTA-MN2 (B). The analyses were performed with a Cosmosil 5C₁₈-PAQ column (4.6 × 250 mm) at a flow rate of 0.6 mL/min with a mixture of water and acetonitrile (92:8) containing 0.1% TFA.

Table 1

In vitro stability of ^{67}Ga -DOTA-MN2 in phosphate-buffered saline (pH 7.4) and mouse plasma at 37 °C

Incubation media	Radiochemical purity (%)				
	1 h	3 h	6 h	12 h	24 h
Phosphate-buffered saline	97.6 ± 2.5	96.5 ± 1.3	96.0 ± 1.0	95.8 ± 0.9	96.4 ± 1.7
Mouse plasma	97.7 ± 0.2	98.0 ± 0.8	96.5 ± 1.2	96.8 ± 0.8	96.2 ± 1.0

Each value represents the mean ± SD of three samples.

Table 2

Biodistribution of radioactivity after intravenous administration of ^{67}Ga -DOTA-MN2 in normal mice

Tissue	Uptake (% injected dose per gram tissue)				
	30 min	1 h	3 h	6 h	24 h
Blood	1.08 ± 0.18	0.42 ± 0.35	0.07 ± 0.06	0.03 ± 0.00	0.01 ± 0.00
Spleen	0.35 ± 0.08	0.14 ± 0.02	0.11 ± 0.04	0.11 ± 0.04	0.02 ± 0.02
Pancreas	0.31 ± 0.05	0.11 ± 0.03	0.09 ± 0.04	0.06 ± 0.07	0.01 ± 0.02
Stomach	0.36 ± 0.07	0.14 ± 0.03	0.09 ± 0.07	0.07 ± 0.05	0.03 ± 0.01
Intestine	0.29 ± 0.05	0.15 ± 0.04	0.09 ± 0.03	0.07 ± 0.03	0.02 ± 0.00
Kidney	4.09 ± 1.02	2.31 ± 0.84	1.51 ± 0.42	0.99 ± 0.18	0.18 ± 0.03
Liver	0.45 ± 0.09	0.22 ± 0.01	0.19 ± 0.03	0.20 ± 0.03	0.07 ± 0.01
Heart	0.48 ± 0.07	0.09 ± 0.01	0.05 ± 0.02	0.02 ± 0.01	0.02 ± 0.02
Lung	0.84 ± 0.13	0.25 ± 0.03	0.09 ± 0.03	0.05 ± 0.01	0.02 ± 0.02
Muscle	0.31 ± 0.03	0.28 ± 0.18	0.16 ± 0.18	0.17 ± 0.16	0.01 ± 0.03
Urine ^a					78.50 ± 4.99
Feces ^a					4.33 ± 2.58

Each value represents the mean ± SD of four animals.

^a Expressed as % injected dose.

was detected in other tissues besides the kidney at any time. The radioactivity level in the kidney was about 4% of the injected dose/g at 30 min post-injection, but it was cleared rapidly from this organ with time. At 24 h post-injection, 79% and 4% of the injected radioactivity of ^{67}Ga -DOTA-MN2 were recovered in the urine and feces, respectively. In cellulose acetate electrophoresis and TLC analyses, more than 85% of the radioactivity excreted in the urine exhibited similar chromatographic behaviors to those of the administered compound, ^{67}Ga -DOTA-MN2 (Fig. 4). The distribution properties of ^{67}Ga -DOTA-MN2 in mice were quite different from those of ^{67}Ga -citrate (Fig. 5). These findings indicate the high in vivo stability and low nonspecific accumulation of ^{67}Ga -DOTA-MN2.

To estimate the tumor accumulation of radioactivity, ^{67}Ga -DOTA-MN2 was administered to NFSa tumor-bearing C3H/He mice (Table 3). This model is widely used in investigations of hypoxic tumors.^{19–22} The normal tissue distributions of ^{67}Ga -DOTA-MN2 in tumor-bearing mice were very similar to those in normal mice. Significant accumulations of the radioactivity in the tumor were observed, and the tumor-to-blood and tumor-to-muscle ratios increased up to 6 h post-injection. Previously, Yang et al. developed a $^{99\text{m}}\text{Tc}$ -labeled metronidazole derivative that $^{99\text{m}}\text{Tc}$ -ethylenedicycysteine chelate was conjugated with two metronidazole moieties.²³ This tracer recognized and identified hypoxic lesions such as tumor hypoxia in rats and infarction areas in patients with acute ischemic stroke.^{23,24} Likewise, the tumor accumulation of ^{67}Ga -DOTA-MN2 would be due to the recognition of the hypoxic lesions by the metronidazole molecules. This is supported by the observation that the tumor accumulation of ^{67}Ga -DOTA-MN2 was significantly higher than that of ^{67}Ga -DOTA (0.23 ± 0.04% injected dose per gram at 1 h postinjection). These results indicate that the drug

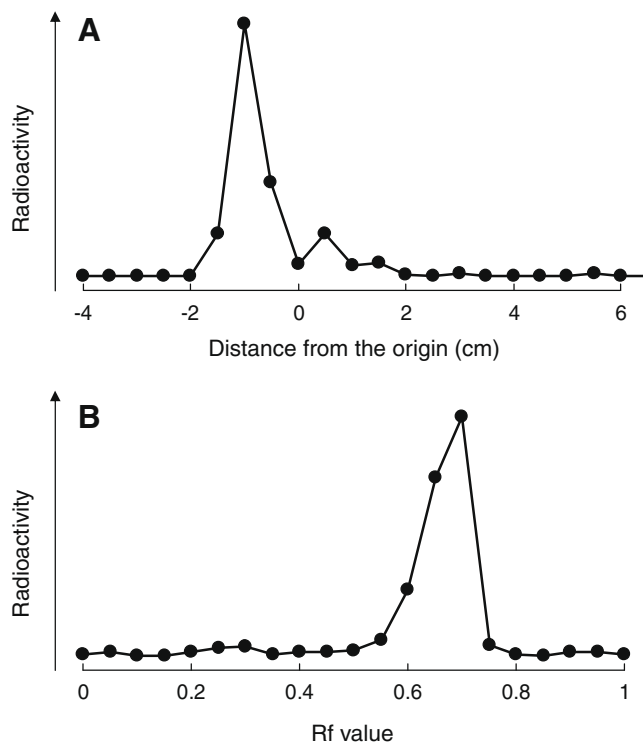


Figure 4. Chromatographic analyses of urine samples for 24 h after injection of ^{67}Ga -DOTA-MN2. These samples were analyzed by cellulose acetate electrophoresis (A) and cellulose F TLC (B). Cellulose acetate electrophoresis was run in an electrostatic field of 0.8 mA/cm for 30 min in veronal buffer ($I = 0.06$, pH 8.6). Cellulose F TLC was developed with a mixture of water, acetonitrile, and 0.1 M citrate (40:60:1). The peak of ^{67}Ga -DOTA-MN2 was observed at 1 cm cathode on cellulose acetate electrophoresis or R_f value of ca. 0.7 on TLC.

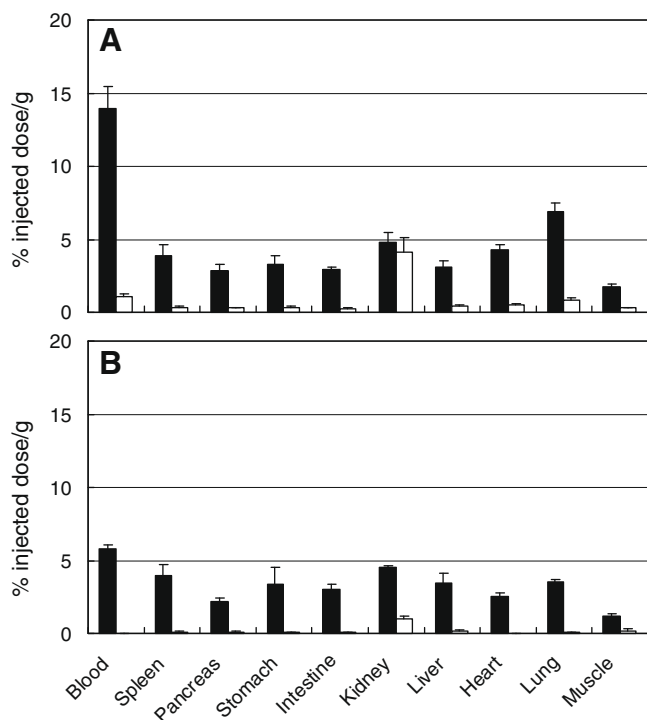


Figure 5. Biodistribution of radioactivity at 30 min (A) and 6 h (B) post-injection of ^{67}Ga -DOTA-MN2 (open columns) or ^{67}Ga -citrate (closed columns) in normal mice. Each value represents the mean \pm SD of four animals.

Table 3
Biodistribution of radioactivity after intravenous administration of ^{67}Ga -DOTA-MN2 in NFSa tumor-bearing C3H/He mice

Tissue	Uptake (% injected dose per gram tissue)		
	1 h	3 h	6 h
Blood	0.59 \pm 0.30	0.06 \pm 0.01	0.05 \pm 0.01
Spleen	0.15 \pm 0.03	0.10 \pm 0.04	0.11 \pm 0.03
Pancreas	0.09 \pm 0.06	0.08 \pm 0.05	0.07 \pm 0.01
Stomach	0.21 \pm 0.10	0.09 \pm 0.02	0.07 \pm 0.02
Intestine	0.37 \pm 0.29	0.09 \pm 0.03	0.06 \pm 0.01
Kidney	2.77 \pm 0.89	1.20 \pm 0.18	1.04 \pm 0.18
Liver	0.25 \pm 0.03	0.15 \pm 0.04	0.20 \pm 0.08
Heart	0.17 \pm 0.13	0.05 \pm 0.04	0.04 \pm 0.01
Lung	0.55 \pm 0.15	0.13 \pm 0.02	0.10 \pm 0.02
Muscle	0.25 \pm 0.13	0.05 \pm 0.01	0.05 \pm 0.03
Tumor	0.49 \pm 0.12	0.22 \pm 0.04	0.20 \pm 0.04
Tumor-to-blood ratio	0.95 \pm 0.30	3.63 \pm 1.10	4.55 \pm 0.44
Tumor-to-muscle ratio	2.36 \pm 0.96	4.05 \pm 0.64	4.42 \pm 1.45

Each value represents the mean \pm SD of four or five animals.

design of ^{67}Ga -DOTA-MN2 based on bifunctional radiopharmaceuticals makes both high in vivo stability of Ga-DOTA chelate and significant recognition of the hypoxic lesions by metronidazole molecules possible.

A specific accumulation of radiotracer in the target tissues is crucial for successful in vivo imaging. For receptor-targeted imaging, ligands with high receptor affinity are prerequisite. Recently, multivalent (bivalent and tetravalent) ligands showed markedly increased binding affinity with their respective receptors compared to monovalent ligands.²⁵ The multivalent concept has been used for the development of receptor-targeted radiotracers.²⁶ The present study suggest that two carboxylate groups of Ga-DOTA complex should be used for coupling to two or more ligand moieties without reducing the complex stability. Furthermore, two different functional moieties would be attached to the Ga-DOTA

complex for multifunctional radiotracers. To explore these ideas, we are currently developing Ga-DOTA-based multivalent ligands and multifunctional tracers.

3. Conclusions

We successfully designed and synthesized a metronidazole-derivatized radiogallium-DOTA chelate, ^{67}Ga -DOTA-MN2, based on the previous findings obtained by X-ray crystallography of Ga-DOTA chelates and the drug design concept of bifunctional radiopharmaceuticals. As expected, ^{67}Ga -DOTA-MN2 exhibited high stability although two carboxylates in the DOTA skeleton were conjugated with metronidazole derivatives. Furthermore, ^{67}Ga -DOTA-MN2 showed not only a significant tumor uptake but also rapid blood clearance and low accumulations in nontarget tissues of the radioactivity after its administration in mice, resulting in the high and increasing target-to-nontarget ratios of the radioactivity. Although further studies are needed, radiogallium-DOTA-MN2 should be a potential radiopharmaceutical for in vivo hypoxia imaging. Also, these results suggest that two functional moieties such as a metronidazole in this study can be conjugated to radiogallium-DOTA chelate without reducing the complex stability. The present findings provide useful information about the chemical design of radiogallium-labeled radiopharmaceuticals for SPECT and PET studies.

4. Experimental

4.1. General procedure

Chemical reagents and solvents were of commercial quality and were used without further purification unless otherwise noted. All melting points were determined on a Yanaco melting point apparatus and are uncorrected. ^1H NMR spectra were obtained on a Varian Unity 400 (400 MHz), and the chemical shifts are reported in parts per million downfield from tetramethylsilane. Infrared (IR) spectra were recorded with a Shimadzu FTIR-8400 spectrometer. High-resolution mass spectra were obtained with an Applied Biosystems Mariner System 5299 spectrometer (ESI MS). Column chromatography was performed on Silica Gel 60N (63–210 μm , Kanto Chemical), and the progress of the reaction was monitored by TLC on Silica Gel 60F 254 plates (Merck). ^{67}Ga was supplied by Fujifilm RI Pharma Co., Ltd. as ^{67}Ga -citrate. Cellulose acetate electrophoresis (Separax-SP) was run in an electrostatic field of 2.5 mA/cm for 20 min or 0.8 mA/cm for 30 min in veronal buffer ($I=0.06$, pH 8.6). Cellulose F TLC was developed with a mixture of water, acetonitrile, and 0.1 M citrate (40:60:1).

4.2. Chemistry

4.2.1. 1,4,7,10-Tetraazacyclododecane-1,4,7,10-tetraacetic acid, 1,7-bis(*tert*-butyl) ester (5)

Compound **5** was prepared in five steps from cyclen according to the literature.¹⁸

4.2.2. Di-*tert*-butyl 2,2'-[4,10-bis(2-{{2-(2-methyl-5-nitro-1H-imidazol-1-yl)ethyl}amino)-2-oxoethyl]-1,4,7,10-tetraazacyclododecane-1,7-diyl]diacetate (6)

1-(2-Aminoethyl)-2-methyl-5-nitroimidazole dihydrochloride was prepared from metronidazole according to the literature.²⁷ Under argon, to a solution of **5** (60.0 mg, 0.12 mmol) in dry $\text{CH}_2\text{Cl}_2/\text{DMF} = 5:1$ (6 mL) was added triethylamine (0.132 mL, 0.93 mmol), 1-(2-aminoethyl)-2-methyl-5-nitroimidazole dihydrochloride (113 mg, 0.47 mmol), HOBt (71.4 mg, 0.47 mmol), and EDC (89.4 mg, 0.47 mmol) in an ice bath. After stirring for 48 h at room

temperature, chloroform (30 mL) was added. The mixture was washed with distilled water, and then dried and evaporated in vacuo. The residue was recrystallized from methanol to obtain **6** (32.3 mg, 33.9%). **6**: White solid; mp 186–189 °C; ¹H NMR (400 MHz, CDCl₃) δ: 1.43 (s, 18H), 2.41 (m, 8H), 2.50 (s, 6H), 2.69 (m, 8H), 3.04 (s, 4H), 3.09 (s, 4H), 3.60 (m, 4H), 4.48 (t, *J* = 6.41 Hz, 4H), 7.93 (s, 2H), 8.58 (m, 2H); IR (KBr) cm⁻¹: 2981, 1743, 1665, 1365, 1261, 1055; ESI MS (*m/z*): 821.4657 (M+H)⁺.

4.2.3. 2,2'-[4,10-Bis(2'-[[2-(2-methyl-5-nitro-1H-imidazol-1-yl)ethyl]amino]-2-oxoethyl)-1,4,7,10-tetraazacyclododecane-1,7-diyl]diacetic acid (**7**) (DOTA-MN2)

A mixture of **6** (17.0 mg, 20.7 μmol) and concd HCl (3.0 mL) was stirred at room temperature for 2 h, and then concentrated in vacuo. After the residue was dissolved in a small amount of methanol, dry ether was added to precipitate **7** (14.0 mg 95.4%). Compound **7**: White solid; mp 152–155 °C; ¹H NMR (400 MHz, D₂O) δ: 2.63 (s, 6H), 3.00–3.20 (m, 16H), 3.60–3.70 (m, 12H), 4.58 (t, *J* = 5.86 Hz, 4H), 8.32 (s, 2H); IR (KBr) cm⁻¹: 3218, 1731, 1681, 1545, 1372, 1195, 1087; ESI MS (*m/z*): 709.3381 (M+H)⁺.

4.2.4. Ga-DOTA-MN2

DOTA-MN2 (1.0 mg, 0.141 mmol) and Ga(NO₃)₃·*n*H₂O (3.0 mg) were dissolved in 0.2 M NH₄OAc buffer (pH 4.6, 0.5 mL). The mixture was stirred and heated at 95 °C for 1 h. After cooling to room temperature, Ga-DOTA-MN2 was purified by HPLC performed with a Cosmosil 5C₁₈-PAQ column (10 × 250 mm) at a flow rate of 3 mL/min with a mixture of water and acetonitrile (90:10) containing 0.1% TFA. ESI MS (*m/z*): 775.2523 (M+H)⁺.

4.2.5. ⁶⁷Ga-DOTA-MN2

To a solution of DOTA-MN2 (50 μg) in 0.2 M NH₄OAc buffer (pH 5.8, 50 μL) was added 30 μL of ⁶⁷Ga-citrate (0.73 MBq). The mixture was stirred and heated at 95 °C for 2 h. After cooling to room temperature, ⁶⁷Ga-DOTA-MN2 was purified by HPLC performed with a Cosmosil 5C₁₈-PAQ column (4.6 × 250 mm) at a flow rate of 0.6 mL/min with a mixture of water and acetonitrile (92:8) containing 0.1% TFA. The radiochemical purity was determined by HPLC, cellulose acetate electrophoresis and cellulose F TLC.

4.3. Biological studies

4.3.1. In vitro stability

⁶⁷Ga-DOTA-MN2 was diluted with 20 mM phosphate-buffered saline (pH 7.4) or mouse plasma, and the solutions were incubated at 37 °C. After 1, 3, 6, 12 and 24 h of incubation, the samples were drawn and the radioactivity was analyzed by cellulose acetate electrophoresis.

4.3.2. Biodistribution study in normal mice

Animal experiments were conducted in accordance with our institutional guidelines and were approved by the Animal Care and Use Committee, Kyushu University. Biodistribution experiments were performed by intravenously administering ⁶⁷Ga-DOTA-MN2 or ⁶⁷Ga-citrate into 6-week-old male ddY mice (28–30 g). ⁶⁷Ga-DOTA-MN2 and ⁶⁷Ga-citrate were diluted with 20 mM phosphate-buffered saline (pH 7.4). Groups of four mice were administered 100 μL of each ⁶⁷Ga-labeled compound (22 kBq) prior to euthanasia at selected time points. Tissues of

interest were removed and weighed, and radioactivity counts were determined with an auto well gamma counter (ARC-370M; Aloka).

4.3.3. Biodistribution study in tumor-bearing mice

Syngeneic NFSa fibrosarcoma cells were inoculated into the right hind leg muscle of female C3H/He mice (5 weeks old). When tumors were approximately 0.5 cm in diameter, the animals were intravenously injected with ⁶⁷Ga-DOTA-MN2 (22 kBq). The biodistribution of radioactivity was monitored at 1, 3 and 6 h post-injection.

Acknowledgments

We would like to thank Fujifilm RI Pharma Co., Ltd, Tokyo, Japan for donating the ⁶⁷Ga-citrate. We also thank Dr. Koichi Ando and Dr. Sachiko Koike of the National Institute of Radiological Sciences, Chiba, Japan for their kind gift of NFSa. This work was supported in part by the Grant-in-Aid for Young Scientists (B) (18790894) from the Ministry of Education, Culture, Sports, Science and Technology of Japan and a Research Grant from the Research Foundation for Pharmaceutical Sciences.

References and notes

- Frick, M. P.; Gupta, N. C.; Sunderland, J. J.; Best, M. A.; Rysavy, J. A.; Shiue, C. Y. *Semin. Nucl. Med.* **1992**, *22*, 182.
- Keppeler, J. S.; Conti, P. S. *Am. J. Roentgenol.* **2001**, *177*, 31.
- Knapp, F. F., Jr.; Mirzadeh, S. *Eur. J. Nucl. Med.* **1994**, *21*, 1151.
- Pagani, M.; Stone-Elander, S.; Larsson, S. A. *Eur. J. Nucl. Med.* **1997**, *24*, 1301.
- Mirzadeh, S.; Lambrecht, R. M. J. *Radioanal. Nucl. Chem.* **1996**, *202*, 7.
- Fani, M.; André, J. P.; Maecke, H. R. *Contrast Media Mol. Imaging* **2008**, *3*, 67.
- Antunes, P.; Ginj, M.; Zhang, H.; Waser, B.; Baum, R. P.; Reubi, J. C.; Maecke, H. *Eur. J. Nucl. Med. Mol. Imaging* **2007**, *34*, 982.
- Zheronosekov, K. P.; Filosofov, D. V.; Baum, R. P.; Aschoff, P.; Bihl, H.; Razbash, A. A.; Jahn, M.; Jennewein, M.; Rösch, F. *J. Nucl. Med.* **2007**, *48*, 1245.
- Win, Z.; Al-Nahhas, A.; Rubello, D.; Gross, M. D. *Q. J. Nucl. Med. Mol. Imaging* **2007**, *51*, 244.
- Benetollo, F.; Bombieri, G.; Calabi, L.; Aime, S.; Botta, M. *Inorg. Chem.* **2003**, *42*, 148.
- Heppeler, A.; Froidevaux, S.; Mäcke, H. R.; Jermann, E.; Béhé, M.; Powell, P.; Hennig, M. *Chem. Eur. J.* **1999**, *5*, 1974.
- Viola, N. A.; Rarig, R. S., Jr.; Ouellette, W.; Doyle, R. P. *Polyhedron* **2006**, *25*, 3457.
- Ogawa, K.; Mukai, T.; Arano, Y.; Hanaoka, H.; Hashimoto, K.; Nishimura, H.; Saji, H. *J. Labelled Compd. Radiopharm.* **2004**, *47*, 753.
- Ogawa, K.; Mukai, T.; Arano, Y.; Ono, M.; Hanaoka, H.; Ishino, S.; Hashimoto, K.; Nishimura, H.; Saji, H. *Bioconjugate Chem.* **2005**, *16*, 751.
- Ogawa, K.; Mukai, T.; Arano, Y.; Otaka, A.; Ueda, M.; Uehara, T.; Magata, Y.; Hashimoto, K.; Saji, H. *Nucl. Med. Biol.* **2006**, *33*, 513.
- Ogawa, K.; Mukai, T.; Inoue, Y.; Ono, M.; Saji, H. *J. Nucl. Med.* **2006**, *47*, 2042.
- Kovacs, Z.; Sherry, A. D. *Synthesis* **1997**, *7*, 759.
- De Leon-Rodriguez, L. M.; Kovacs, Z.; Esqueda-Oliva, A. C.; Miranda-Olvera, A. D. *Tetrahedron Lett.* **2006**, *47*, 6937.
- Halpern, H. J.; Yu, C.; Peric, M.; Barth, E.; Grdina, D. J.; Teicher, B. A. *Proc. Natl. Acad. Sci. U.S.A.* **1994**, *91*, 13047.
- Ando, K.; Koike, S.; Ohira, C.; Chen, Y. J.; Nojima, K.; Ando, S.; Ohbuchi, T.; Kobayashi, N.; Shimizu, W.; Urano, M. *Int. J. Radiat. Biol.* **1999**, *75*, 505.
- Yamamoto, F.; Aoki, M.; Furusawa, Y.; Ando, K.; Kuwabara, Y.; Masuda, K.; Sasaki, S.; Maeda, M. *Biol. Pharm. Bull.* **2002**, *25*, 616.
- Mahy, P.; De Bast, M.; Gillart, J.; Labar, D.; Grégoire, V. *Eur. J. Nucl. Med. Mol. Imaging* **2006**, *33*, 553.
- Yang, D. J.; Ilgan, S.; Higuchi, T.; Zareneyrizi, F.; Oh, C. S.; Liu, C. W.; Kim, E. E.; Podoloff, D. A. *Pharm. Res.* **1999**, *16*, 743.
- Song, H. C.; Bom, H. S.; Cho, K. H.; Kim, B. C.; Seo, J. J.; Kimm, C. G.; Yang, D. J.; Kim, E. E. *Stroke* **2003**, *34*, 982.
- Kiessling, L. L.; Gestwicki, J. E.; Strong, L. E. *Angew. Chem., Int. Ed.* **2006**, *45*, 2348.
- Liu, S. *Mol. Pharm.* **2006**, *3*, 472.
- Hay, M. P.; Wilson, W. R.; Moselen, J. W.; Palmer, B. D.; Denny, W. A. *J. Med. Chem.* **1994**, *37*, 381.